Nanoscale

PAPER

View Article Online
View Journal | View Issue

Open Access Article. Published on 06 July 2015. Downloaded on 7/19/2025 11:24:58 PM.
This article is licensed under a Creative Commons Attribution 3.0 Unported Licence.

Cite this: *Nanoscale*, 2015, **7**, 13511

Differentiating sepsis from non-infectious systemic inflammation based on microvesicle-bacteria aggregation†

I. K. Herrmann,*[a] S. Bertazzo,[a] D. J. P. O'Callaghan,[b] A. A. Schlegel,[c] C. Kallepitis,[a] D. B. Antcliffe,[b] A. C. Gordon[b] and M. M. Stevens*[a]

Received 23rd March 2015,
Accepted 30th June 2015

DOI: 10.1039/c5nr01851j

www.rsc.org/nanoscale

Sepsis is a severe medical condition and a leading cause of hospital mortality. Prompt diagnosis and early treatment has a significant, positive impact on patient outcome. However, sepsis is not always easy to diagnose, especially in critically ill patients. Here, we present a conceptionally new approach for the rapid diagnostic differentiation of sepsis from non-septic intensive care unit patients. Using advanced microscopy and spectroscopy techniques, we measure infection-specific changes in the activity of nano-sized cell-derived microvesicles to bind bacteria. We report on the use of a point-of-care-compatible microfluidic chip to measure microvesicle-bacteria aggregation and demonstrate rapid (≤1.5 hour) and reliable diagnostic differentiation of bacterial infection from non-infectious inflammation in a double-blind pilot study. Our study demonstrates the potential of microvesicle activities for sepsis diagnosis and introduces microvesicle-bacteria aggregation as a potentially useful parameter for making early clinical management decisions.

Introduction

Sepsis is the presence of the systemic inflammatory response syndrome (SIRS) due to infection and represents a potentially life-threatening condition. It remains a major cause of morbidity and is currently the tenth most common cause of death overall.[1–3] The management of sepsis is technically demanding and costly, translating to an associated annual multibillion dollar burden for the healthcare industry.[4]

There is compelling evidence that early diagnosis of sepsis is key to improved patient outcomes.[5,6] The majority of intensive care unit (ICU) patients exhibit signs of systemic inflammation and up to 93% meet the SIRS criteria at some point during their ICU stay, yet discriminating a sepsis patient needing antibiotic treatment from one with non-infectious SIRS remains challenging.[2] Blood cultures require long incubation times (>24 hours) and have a high incidence of false negatives.[7] As a result, making early clinical management decisions according to blood culture assays is not always possible. To help guide treatment, research efforts have focused on surrogate markers of inflammation; large numbers have been investigated, but few have entered routine clinical application.[8] Those that are used (*e.g.*, C-reactive protein (CRP), procalcitonin (PCT)) are not always able to consistently discriminate patients with sepsis from those with non-infectious SIRS.[8–10] Diagnostic uncertainty makes it difficult for clinicians to determine when to provide or withhold antibiotic treatment.[5] Failing to provide appropriate antibiotics results in increased morbidity and mortality, whereas excessive use results in increased bacterial resistance. Antibiotic resistant bacteria is a major global healthcare challenge, along with side-effects such as *Clostridium difficile* diarrhoea.[11]

Recently, leukocytes have been shown to release trigger-dependent microvesicle subpopulations in response to bacterial exposure. Microvesicles are nano-sized membrane-bound fragments released from cells under both physiological and pathological conditions, with their composition varying according to both the cell type and the eliciting stimulus.[12–19] Timár *et al.*[15] recently investigated the release of microvesicles from neutrophils *in vitro* under physiological conditions and in response to various triggering substances and found that microvesicles derived from neutrophils exposed to *Staphylococcus aureus* (*S. aureus*), showed distinct aggregation with exogenously added bacteria while significantly less aggregation was observed with microvesicles from neutrophils not exposed to bacteria. While there is increasing evidence that microvesi-

[a]*Department of Materials, Department of Bioengineering and Institute of Biomedical Engineering, Imperial College London, Prince Consort Road, London, SW7 2AZ, UK. E-mail: ingekherrmann@gmail.com, m.stevens@imperial.ac.uk*
[b]*Anaesthetics, Pain Medicine and Intensive Care, Department of Surgery and Cancer, Imperial College London, Charing Cross Hospital, Fulham Palace Road, London, W6 8RF London, UK*
[c]*Swiss HPB and Transplantation Center, Department of Surgery, University Hospital Zurich, Rämistrasse 100, CH-8091 Zurich, Switzerland*

†Electronic supplementary information (ESI) available: Fig. S1: Markers of inflammation and microvesicle characteristics in patient plasma samples, Fig. S2: Experimental sepsis model, Table S1: Patient characteristics. Table S2: Inclusion/exclusion criteria. See DOI: 10.1039/c5nr01851j

Open Access Article. Published on 06 July 2015. Downloaded on 7/19/2025 11:24:58 PM.
This article is licensed under a Creative Commons Attribution 3.0 Unported Licence.

cles undergo specific phenotypic changes in response to triggers,[15,16] little is known about their diagnostic potential.

In this study, we investigated the diagnostic potential of functional microvesicle activity in sepsis using plasma samples from ICU patients suffering from non-infectious SIRS or sepsis. Moreover, we present a microfluidic chip that allows semi-quantitative readouts of microvesicle activity and opens up the possibility of implementing microvesicle activity assays into a clinically applicable platform for the rapid diagnostic differentiation of (bacterial) sepsis from non-infectious inflammation.

Results

Microvesicle release from polymorphonuclear cells (PMNs) in response to bacteria *in vitro*

To characterize the formation of polymorphonuclear cell (PMN)-derived microvesicles in response to different bacterial triggers, we studied the process of microvesicle shedding from PMNs in response to two of the most common etiologic agents in sepsis, *S. aureus* (Gram-positive) and *Escherichia coli* (*E. coli*) (Gram-negative), and lipopolysaccharide (LPS) *in vitro*. Characterization of supernatants by scanning electron microscopy (SEM) confirmed the presence of microvesicles and Nanoparticle Tracking Analysis (NTA) showed increased concentration of microvesicles in PMN samples exposed to serum-opsonised *S. aureus, E. coli* and heat-inactivated *S. aureus* bacteria (bioparticles), with comparable microvesicle size distributions between 50 and 800 nm (Fig. 1a and b). Microvesicles were stained for neutrophil markers (double staining for CD11β/CD18 and CD11β/CD177). CD11β/CD18 and CD11β/CD177-double positive microvesicles were found to be elevated by a factor of ~4 compared to control samples in PMNs exposed to *S. aureus* ($p < 0.01$), and elevated by a factor of ~2.5 and ~4 in PMNs exposed to *E. coli* ($p < 0.01$), respectively (Fig. 1c). While LPS did not significantly affect the concen-

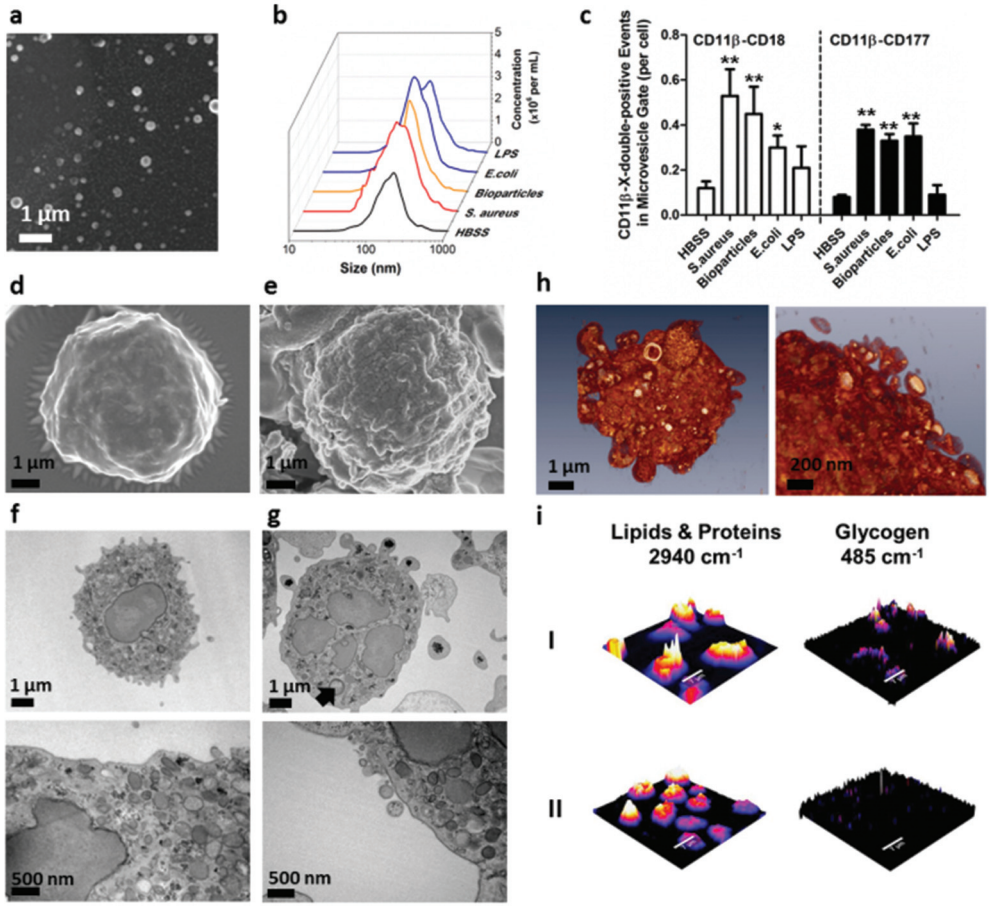

Fig. 1 Trigger-dependent microvesicle shedding. Scanning electron micrograph (a) and size-distribution assessed by NTA (b) of PMN-derived microvesicles originating from PMNs incubated with plasma-opsonized *S. aureus* bacteria, *E. coli*, LPS, heat-inactivated bacteria bioparticles or vehicle (HBSS). PMN-derived CD11β/CD18 and CD11β/CD177-double positive events assessed by flow cytometry as a function of bacterial triggering agent ($n = 3$) (c). Scanning (d,e) and transmission electron micrographs (f,g) of PMNs showing pronounced membrane budding and shedding of microvesicles following incubation with opsonised *S. aureus* particles for 30 minutes (arrow indicates *S. aureus* particle) (e,g) compared to PMNs incubated with HBSS (d,f). 3D-Tomographies and outer surface reconstructions of PMN incubated with *S. aureus* further confirmed the constriction of vesicles from the outer membrane seen in TEM (h). Raman spectroscopy maps of PMN incubated with (top, I) or without (bottom, II, control) bacteria showed lipid droplets and *peri*-membranous accumulation of glycogen granules in stimulated PMNs (I) compared to control (II) (i).

 This journal is © The Royal Society of Chemistry 2015

Open Access Article. Published on 06 July 2015. Downloaded on 7/19/2025 11:24:58 PM.
This article is licensed under a Creative Commons Attribution 3.0 Unported Licence.

tration of CD11β-positive microvesicles, heat-inactivated *S. aureus, E. coli* and bioparticles showed comparable effects to live bacteria. Together, these *in vitro* results suggested that microvesicle release was triggered by the presence of opsonised (bacteria) particles.

We next characterized the process of microvesicle shedding from PMNs *in vitro* using advanced electron microscopy and spectroscopy techniques. Microvesicle release was evaluated in samples prepared by incubating isolated human PMNs with or without serum-opsonized *S. aureus* for 30 minutes. Scanning electron micrographs showed pronounced membrane budding in PMNs exposed to *S. aureus* compared to resting PMNs (Fig. 1d and e). Transmission electron micrographs of thin sections of PMNs containing phagocytised *S. aureus* bacteria confirmed increased membrane budding and formation of microvesicles (Fig. 1f and g). Formation of glycogen granule clusters, translocation and *peri*-membranous massing of glycogen granule aggregates, and shipping of cytoplasmatic microvesicles containing glycogen granules were observed in PMNs exposed to bacteria, while glycogen granules remained well-dispersed in the cytoplasm of unstimulated PMNs (Fig. 1f and g). 3D-Tomography of PMNs further confirmed constriction of vesicular structures from the cellular membrane (Fig. 1h). Confocal Raman spectroscopy maps showed glycogen granule aggregation (Raman shift of glycogen[20]: 485 cm^{-1}) in response to *S. aureus* exposure (Fig. 1i). While very few glycogen clusters were detectable in control samples, which indicated that the 20 nm granules remained well dispersed, glycogen clusters were detected in samples exposed to *S. aureus*, mostly in *peri*-membranous regions. These findings indicated that exposure of PMNs to bacteria led to *peri*-membraneous accumulation of glycogen (as previously reported by Robinson *et al.*[21]) and the shedding of microvesicles enriched in glycogen.

Characterization of microvesicles in plasma samples from sepsis and SIRS patients

In order to assess the *in vivo* relevance and diagnostic potential of PMN-derived microvesicles in differentiating bacterial sepsis from non-infectious SIRS, we analysed heparinised plasma samples from 22 brain-injured ICU patients (patient characteristics, see ESI Table S1†). The plasma samples had been collected within 72 hours of ICU admission. Twelve patients had non-infectious SIRS (SIRS criteria ≥2) as part of their underlying condition. Two patients presented with SIRS criteria <2 and eight patients were diagnosed with sepsis (6 patients) or suspected sepsis (2 patients) based on their clinical presentation (SIRS criteria ≥2) and blood culture results. Among the sepsis patients with positive blood culture, three patients had a Gram-positive blood culture and three patients had a Gram-negative blood culture. For statistical analysis, patients with SIRS criteria <2 and non-infectious SIRS patients were classified as control group (n = 14) while patients with known or suspected sepsis were classified as sepsis group (n = 8). Analysis of clinical data based on the SIRS criteria showed no significant differences between the control and sepsis groups (see ESI Table S1†). Commonly used concentrations of sepsis biomarkers such as C-reactive protein (CRP, p = 0.081, β = 0.7) and procalcitonin (PCT, p = 0.056, β = 0.84) showed no differences between the two groups, although statistical power was limited (ESI Fig. S1a and b†).

Microvesicle populations were isolated from plasma by ultracentrifugation (100 000*g* for 1 hour at 4 °C) and characterized by NTA and flow cytometry. No difference in microvesicle size or concentration was found between the sepsis and control groups by NTA (ESI Fig. S1c and d†). Both CD11β/CD18 and CD11β/CD177-double positive microvesicle concentrations were elevated in the sepsis group compared to the control group (CD11β/CD18-double positive microvesicles, p = 0.01, β = 0.40; CD11β/CD177-double positive microvesicles, p = 0.008, β = 0.28) (ESI Fig. S1e†).

Functional activity of plasma-derived microvesicles in SIRS and sepsis patients

We characterized microvesicle plasma populations in clinical samples according to three characteristic processes altered during sepsis: inflammation, procoagulant activity, and bacteria aggregation activity. The proinflammatory, procoagulant and aggregation activity of isolated microvesicles were measured and evaluated regarding their sensitivity and specificity for sepsis diagnosis (Fig. 2a). First, the inflammatory phenotype of the microvesicle isolates was determined in an endothelial cell-based assay for both sepsis and control patients. Human endothelial cells were exposed to patient plasma-derived microvesicles for 24 hours and the release of Lactate Dehydrogenase (LDH, indicative for cell death) and Interleukin-6 (IL-6) was quantified. No microvesicle-induced cell death was observed (Fig. 2a and b). While exposure of endothelial cells to plasma-derived microvesicles led to slightly elevated IL-6 protein levels (2-fold increase relative to cells not exposed to microvesicles, p = 0.03), we detected no significant difference between the inflammatory activity of microvesicles from sepsis and control group patients (Fig. 2c). The inflammatory activity of both microvesicle populations was low compared to the IL-6 expression in LPS-stimulated endothelial cells (7-fold increase of IL-6 protein expression, p < 0.01). Cytokine levels (Interleukin-1α, IL-6, and Tumour Necrosis Factor-α) in microvesicle isolates were below assay detection limits (<10 pg mL^{-1}).

Microvesicle procoagulant activity in patient plasma samples was measured based on phospholipid-mediated thrombin activation (Fig. 2a and d). Additionally, plasma clotting time was measured by adding microvesicles isolated from patient samples to re-calcified microvesicle-depleted citrated plasma and then measuring turbidity change due to fibrinogen-fibrin polymerization (Fig. 2a and e). We observed that the procoagulant activity of the microvesicle population in the sepsis group was elevated (p = 0.04, β = 0.45). In keeping with the higher procoagulant activity of microvesicles, plasma clotting time was shortened in those samples exposed to microvesicles from septic patients (p = 0.04, β = 0.16).

Finally, we measured bacteria aggregation activity of plasma-derived microvesicles. Patient plasma-derived micro-

Open Access Article. Published on 06 July 2015. Downloaded on 7/19/2025 11:24:58 PM.
This article is licensed under a Creative Commons Attribution 3.0 Unported Licence.

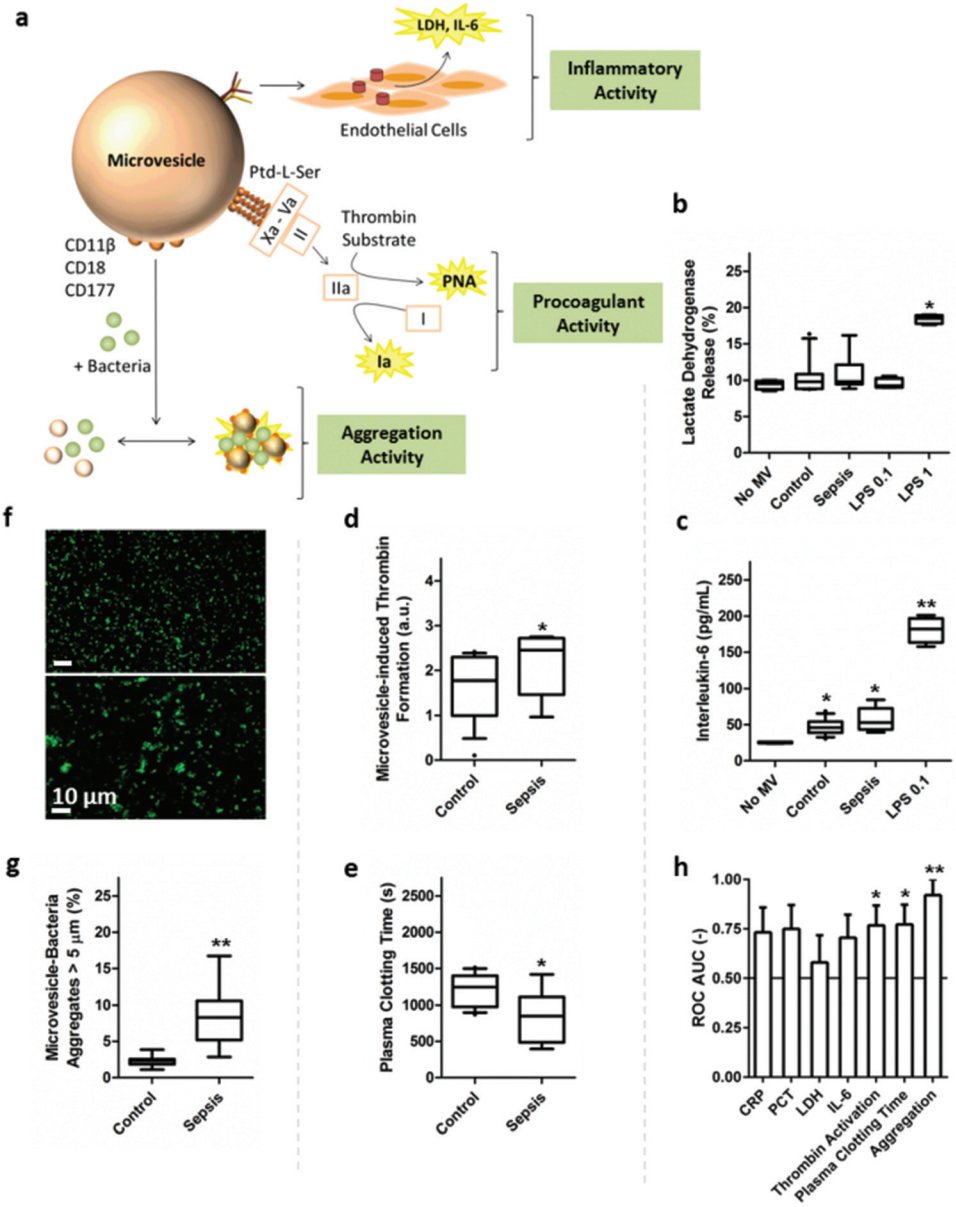

Fig. 2 Microvesicle-based functional activity in clinical samples. Microvesicle-induced cell-death and inflammatory response in an endothelial cell model (a). Lactate dehydrogenase (LDH) release (indicative for cell death) (b) and interleukin-6 expression (c) of endothelial cells in response to microvesicle exposure for 24 hours. Microvesicle procoagulant activity was measured by assessing phosphatidylserine-induced thrombin activation (a,d) and microvesicle-induced changes in plasma clotting time in re-calcified plasma (a,e). Microvesicle-triggered bacteria aggregation (a). Bacteria aggregate size was quantified for control group and sepsis patient microvesicle isolates after incubation with stained (green) *S. aureus* bacteria based on confocal fluorescence image analysis (f,g). Corresponding receiver operating characteristic area under the curve values for commonly used biomarkers (C-reactive protein (CRP), Procalcitonin (PCT)) and microvesicle activites (h).

vesicles were incubated with a stained *S. aureus* bacteria standard and bacteria-microvesicle aggregation was measured by counting aggregates larger than 5 µm using confocal microscopy (Fig. 2a and f). The number of large bacteria aggregates was significantly higher in sepsis patient samples compared to controls ($p < 0.01$, $\beta = 0.07$) (Fig. 2g).

Receiver Operating Characteristics (ROC) with corresponding area under the curve values (AUC) were calculated for clinically used sepsis biomarkers (CRP and PCT) and microvesicle characteristics (Fig. 2h); the closer AUC is to 1, the better the diagnostic performance. ROC analyses of the control *versus* the sepsis group showed significantly different AUC values for both coagulation assays (procoagulant activity assay: AUC = 0.78 ± 0.10, $p = 0.04$; plasma clotting time assay: AUC = 0.74 ± 0.11, $p = 0.04$). ROC analysis of the bacteria aggregation assay resulted in an AUC value of 0.92 ± 0.08 ($p < 0.01$). Posi-

 This journal is © The Royal Society of Chemistry 2015

Open Access Article. Published on 06 July 2015. Downloaded on 7/19/2025 11:24:58 PM.
This article is licensed under a Creative Commons Attribution 3.0 Unported Licence.

tive correlations were found between CD11β-CD18-double positive microvesicles and bacteria-aggregation (Spearman's rho: 0.41, $p = 0.049$) as well as CD11β-CD177-double positive microvesicles and aggregation (Spearman's rho: 0.45, $p = 0.033$).

Microvesicle activity in blood plasma from an experimental sepsis animal model

In order to better understand the relevance of microvesicles during sepsis progression and evaluate whether microvesicle aggregation could serve as an early sepsis marker, we evaluated microvesicle concentration and aggregation activity of plasma-derived microvesicles in a standard rat model of polymicrobial septic peritonitis (Fig. 3a). We analysed plasma samples collected before caecal ligation and puncture (CLP)[22,23] surgery and every 24 hours for up to 96 hours. The overall survival in the CLP group was 75% (ESI Fig. S2a†) and a distinct weight loss up to 7% was observed in the CLP group in the first 24 hours ($p < 0.01$) (ESI Fig. S2b†). The concentration and size of microvesicles isolated from plasma were in the same order as for the patient plasma samples and no significant difference between the SHAM and the CLP group was found in terms of size or concentration at any of the time points. The plasma concentration of CD11β/CD18-double positive microvesicles was increased in the CLP-group, which reached peak concentrations at 48 hours and then gradually decreasing to values comparable to baseline 96 hours after sepsis induction (Fig. 3b). Aggregation activity in samples was significantly different between the SHAM and the CLP group with an AUC (t_{24}) = 0.76 ± 0.11, ($p = 0.041$) at 24 hours and an AUC (t_{48}) = 0.89 ± 0.09, ($p < 0.01$) at the 48 hour time point (Fig. 3c and d). Again, aggregation activity significantly correlated with CD11β/CD18-double positive microvesicles (Spearman's rho: 0.72, $p < 0.01$).

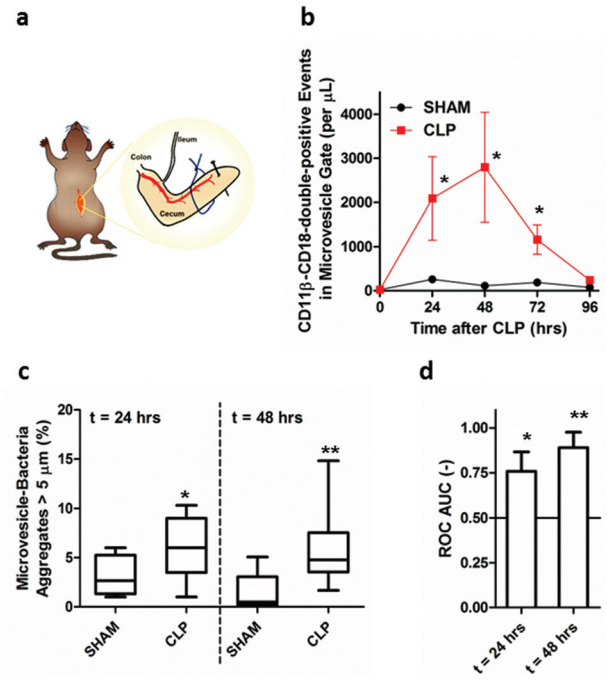

Fig. 3 Microvesicles in plasma samples from an experimental sepsis model. Caecal ligation and puncture (CLP) procedure in rats (a). Time-dependent concentration of neutrophil-derived CD11β/CD18-double positive microvesicles assessed by flow cytometry (b). Aggregation of *S. aureus* bacteria standard with microvesicle isolates from animal plasma at the 24 and 48 hour time point (c) and corresponding ROC curves (d).

Characterization of microvesicle-bacteria aggregates

In order to better understand the nature of the microvesicle-bacteria aggregates, we used an *in vitro* analysis to further characterize their properties. The CD11β-positivity of the aggregating human PMN-derived vesicles was confirmed by immunostaining (Fig. 4a) and transmission electron micrographs of microvesicle-bacteria aggregates were recorded (Fig. 4b). The microvesicle-concentration dependence of bacteria aggregation was confirmed by serially diluting microvesicle isolates from PMNs exposed to *S. aureus* (*in vitro*). If microvesicle isolates were diluted with HBSS (1 : 10), no significant aggregation was detected, while microvesicle isolates incubated with bacteria at their original concentration (or if they became concentrated by ultracentrifugation) showed more pronounced aggregation (Fig. 4c).

Microfluidic chip to measure aggregation activity

Based on the results of the aggregation activity, we developed a microfluidic chip that allowed semi-quantitative assay readouts of aggregation activity. We used heat-inactivated serum-opsonized *S. aureus* bioparticles as the aggregation agent. Following the incubation of bioparticles with different concentrations of PMN-derived microvesicles, the sample was filtered through a weir-filter chip. The performance of a microfluidic weir-filter chip with slits of 5, 10 and 20 µm was evaluated for the separation of aggregated bacteria. Fluorescence intensity was measured at the inlet and outlet of the chip and was indicative of the degree of sample aggregation (Fig. 4d). While the 5 µm slit chip demonstrated significant clogging, the 10 µm slit filter allowed separation of bioparticle aggregates from single bioparticles. The degree of aggregation, as determined by the ratio of the fluorescence intensity at the inlet and outlet, correlated well with the image analysis and the microvesicle concentration (Spearman's rho 0.87, $p < 0.05$) (Fig. 4e).

For validation purposes, a blinded trial was performed including 6 samples from a temporally different set of patients. A total of 12 samples (from 6 sepsis patients and 6 non-infectious SIRS patients) were analysed in the blinded trial using a weir-filter chip with a slit height of 10 µm. We found that 10 out of 12 samples were assigned to the correct group (based on clinical diagnosis). With a cut-off value of 0.9 for the chip fluorescence readout (outlet/inlet), one sample was false positive and one sample was borderline (with a value of 0.89) (Fig. 4f). The correlation between the chip readout and the CD11β-CD177-double positive microvesicle concentration was −0.67 ($p < 0.05$).

Open Access Article. Published on 06 July 2015. Downloaded on 7/19/2025 11:24:58 PM.
This article is licensed under a Creative Commons Attribution 3.0 Unported Licence.

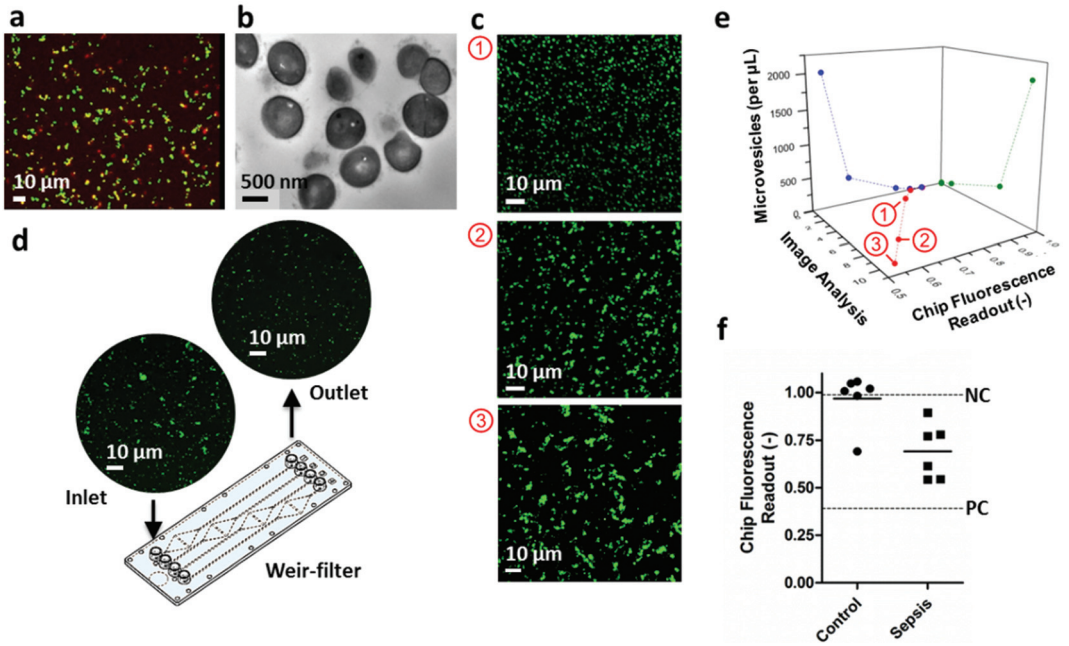

Fig. 4 Microvesicle-bacteria aggregation – characterization and microfluidic chip assay. Confocal images of stained *S. aureus* bacteria before and after incubation with PMN-derived microvesicles showed co-localization of CD11β-stained microvesicles (red) with aggregated bacteria (green) (a). Transmission electron micrograph of aggregated bacteria (b). Increasing the microvesicle concentration lead to more pronounced bacteria aggregation (low (1), intermediate (2) and high (3) microvesicle concentration) (c). Geometry of the weir-type filter microfluidic chip with four separation channels (d). Correlation of the change in fluorescence intensity (outlet/inlet, *x*) of the chip and results from image analysis (*y*) and microvesicle concentration measurements (*z*) (e). Results from the blinded test showing chip readouts for the control (n = 6) and sepsis (n = 6) patients, and readouts of the negative control (NC) and positive control (PC) using a weir-filter chip with a 10 µm slit (f).

Discussion

This is the first study investigating the diagnostic potential of PMN-derived microvesicles for the differentiation of infectious (sepsis) and non-infectious systemic inflammation. We found that exposure of PMNs to Gram-negative and Gram-positive bacteria induced significant shedding of distinct microvesicle populations with increased bacteria aggregation activity and high specificity towards infection in experimental as well as clinical settings. This study corroborates and validates increasing evidence that microvesicles undergo stimulus-dependent phenotypic changes, and paves the way for microvesicle-based diagnostics.[19,24]

While differences in clinical parameters and biomarker concentrations between sepsis patients and healthy volunteers are often pronounced, discriminating patients with sepsis from those with non-infectious SIRS remains challenging. We found the proinflammatory activity of microvesicles was comparable across the patient groups, but the procoagulant and aggregation activities of microvesicles were significantly increased in sepsis. In particular, aggregation activity showed a high specificity and sensitivity to infection over inflammation in our small, heterogeneous patient cohort (which included Gram-negative, Gram-positive, and possibly polymicrobial infections).

Together with the findings from Timár *et al.*[15] and Oehmcke *et al.*,[16] our results strongly suggest that there is an infection-specific shift in microvesicle properties that lead to increased aggregation activity. Since this increased aggregation activity is initiated by the innate immune system in response to infection rather than inflammation, this activitiy may facilitate the early differentiation of non-infectious and infectious inflammatory processes. The results obtained in the murine sepsis model suggested an increase of circulating leukocyte-derived microvesicles already in the early phase of sepsis, which reached values comparable to baseline once abscess formation in CLP animals was under control, and which coincided with the stabilization of body weight. The PMN-derived microvesicle isolates from animal plasma samples showed similar aggregation activity and specificity/sensitivity for infection as previously observed for clinical samples, which suggested that these phenomena are a collectively preserved response to early sepsis. Our microfluidic chip opens up the possibility of evaluating microvesicle activity in a clinical setting for the rapid diagnostic differentiation of (bacterial) sepsis from non-infectious inflammation.

Conclusions

In conclusion, our study demonstrates the use of microvesicle-based functional activities for the rapid (≤1.5 hour) diagnosis of sepsis. Our assay serves as a potentially attractive complementary test to currently-used inflammation-based surrogate

 This journal is © The Royal Society of Chemistry 2015

Open Access Article. Published on 06 July 2015. Downloaded on 7/19/2025 11:24:58 PM.
This article is licensed under a Creative Commons Attribution 3.0 Unported Licence.

markers or blood cultures in making early clinical management decisions regarding the administration of antibiotics. This is particularly important as antibiotic resistance rates have increased over the last decade and resistant microbes have been identified as a major global healthcare challenge.[25,26] Additionally, our findings further support the supposition that the development of diagnostic assays for sepsis may require exploring new avenues, including probing of the cellular response and degree of cell activation, *e.g.*, by analysing nano-sized cell-derived vesicles. The developed microfluidic weir-filter chip provides a platform that opens microvesicle aggregation to evaluation in a large patient cohort in real time; in a larger cohort, potentially confounding factors such as patient heterogeneity, neutropenia, surgery and trauma injury, and masking due to (antibiotic) therapy can also be examined. While our study is based on a small patient number, the good diagnostic performance in both an experimental sepsis model and an unselected, heterogeneous ICU patient set suggests future potential for microvesicles as infection-specific markers.

Experimental

Study approval

Ethical approval was given (North London REC 3 reference: 10/H0709/77). Written informed consent was received from participants prior to inclusion in the study. Previously collected samples from 28 patients were analysed. Patient characteristics and inclusion/exclusion criteria can be found in the ESI Tables S1 and S2.† Animal studies were conducted in accordance with the Institutional Animal Care and Use Committee (approved by the veterinary office of Zurich, Switzerland, 14/2011).

Polymorphonuclear cell isolation

PMNs were isolated from healthy volunteers following previously described procedures.[27] Briefly, 20 mL of blood was drawn using acid citrate dextrose (ACD, Sigma Aldrich) as anticoagulant. Red blood cells were lysed using red blood cell lysis buffer (10 mM $KHCO_3$, 155 mM NH_4Cl (both from Sigma Aldrich) in Milli-Q water (18 MΩ, sterile filtered) and white blood cells were pelleted by centrifugation at 350*g* for 10 minutes. White blood cells were then layered on a Ficoll gradient (Histopaque 1077, Sigma Aldrich) and centrifuged for 30 minutes at 350*g*. Flow cytometry confirmed >95% of the isolated cells were CD11β-positive. PMN *in vitro* experiments were repeated at least three times with three different batches of PMNs ($n \geq 3$).

Bacteria and lipopolysaccharide

Staphylococcus aureus subsp. *aureus Rosenbach* (*S. aureus*, ATCC 29213) bacteria were cultured in suspension in Tryptic Soy broth (Sigma Aldrich) and *Escherichia coli (Migula) Castellani and Chalmers* (*E. coli* ML35, ATCC 43827)) were cultured in LB broth (Sigma Aldrich) in an incubator at 37 °C on a shaker (250 rpm). Heat-inactivated bacteria were prepared by incubating the bacteria suspension at 90 °C for 1 hour. For experiments, bacteria and bacteria bioparticles (LifeTechnologies) were washed in HBSS and opsonised with human serum (from human male AB plasma, sterile filtered, Sigma Aldrich) for 30 minutes at 37 °C following the protocol by Timár *et al.*[15] After opsonisation, bacteria were washed with HBSS. The stock concentration was set to $OD_{600} \sim 1$ for bacteria and to 10^9 per mL for bioparticles. Lipopolysaccharide (from *E. coli* 055:B5, Sigma Aldrich) was dissolved in PBS at a stock concentration of 10 mg mL^{-1} and further diluted as needed.

Microvesicle characterization – *in vitro* samples

Freshly isolated human PMNs were then incubated with opsonised bacteria for 30 minutes and supernatants were collected for further analysis (100 000*g* for 1 hour at 4 °C, Beckman Ultracentrifuge). Microvesicles were characterized by NTA (LM10, Nanosight) and Flow Cytometry (Fortessa, BD Biosciences). For NTA measurements, microvesicles were measured directly or diluted 1 : 10 in triple-filtered HBSS where necessary. The same camera settings (camera level 13) were used for all measurements and each sample was measured at least three times. For flow cytometry, microvesicles were either analyzed unstained or double-stained with leukocyte antibodies (CD11β, CD177 or CD18). For staining, FITC-conjugated anti-human-CD177 (MEM-166, Mouse IgG1, Abcam) or FITC-conjugated anti-human-CD18 (TS1/18, Mouse IgG1, κ, BioLegend) and Alexa-647-conjugated anti-human-CD11β antibodies (M1/70, Rat IgG2b, κ, BioLegend) were used at concentrations of 1 μg mL^{-1} (1 hour, 37 °C in the dark) and double positive events were counted in the microvesicle gate (events ≤1 μm beads) using counting beads (CountBright, LifeTechnologies). Isotype controls and differential TritonX lysis (0.1% v/v) were used to exclude non-specific binding and binding to non-vesicular substructures (protein aggregates, *etc.*).[28]

Electron micrographs

S. aureus bacteria were opsonised with human serum (human serum, Sigma Aldrich). Freshly isolated PMN were incubated with serum-opsonized *S. aureus* bacteria for 30 minutes at 37 °C. Following incubation, supernatants were collected for further analysis, and cells were re-suspended and fixed with 4% v/v paraformaldehyde (PFA, 16% v/v Paraformaldehyde aqueous solution, Electron Microscopy Sciences, Hatfield, PA, diluted in PBS) and 0.2% v/v glutaraldehyde (Grade II, 25% v/v in H_2O, Sigma Aldrich, diluted in PBS) for 12 hours and centrifuged at 3000*g* for 10 minutes. For SEM, samples were dehydrated with ethanol (30% v/v, 50%, 70%, 90%, 100% (3×), 5 minutes each), re-suspended in hexamethyldisilazane (HMDS, Sigma Aldrich) and dried on a glass cover slip. Samples were secured to an aluminium sample holder with carbon tape, and silver paint was applied to the area immediately surrounding each sample, which was then coated with 5 nm carbon (Quorum Technologies Turbo-Pumped Thermal Evaporators model K975X) and 5 nm chromium in a sputter coater (Quorum Technologies Sputter Coater model K575X). Following the coating procedure, samples were imaged by SEM (Gemini 1525 FEGSEM), operated at 5 kV.

Open Access Article. Published on 06 July 2015. Downloaded on 7/19/2025 11:24:58 PM.
This article is licensed under a Creative Commons Attribution 3.0 Unported Licence.

For TEM and 3D tomography, samples were fixed in a 4% (v/v) formaldehyde (Sigma, BioReagent, ≥36.0%) with 0.2% (v/v) glutaraldehyde (EMS [Electron Microscopy Sciences]) solution in PBS at room temperature for 15 minutes. Samples were washed three times with cacodilate buffer (EMS) and osmicated with osmium tetroxide in 2% (w/v) cacodilate buffer for 30 minutes. After that, samples were washed five times with deionized water and then dehydrated through a graded ethanol (Sigma, ACS reagent 99.5%) series two times for each concentration (20, 30, 40, 50 70, 80, 90, 100, 100, 100% (v/v)) for 5 minutes in each solution. After dehydration, samples were infiltrated with Epon Resin (EMS) diluted in ethanol at 3 : 1, 2 : 1, and 1 : 1 for 1 hour each, and then overnight at 1 : 2. The solution was then replaced with pure resin, which was changed twice in the first 12 hours and then allowed to infiltrate again overnight. Samples were placed in an oven at 60 °C and left to cure overnight. Cured resin blocks were sectioned at 100 nm in an ultramicrotome (Leica) and immediately placed on carbon-coated copper grids. The grids were imaged in the TEM at 80 kV (JEOL 2000FX TEM).

Resin blocks were also secured to a SEM aluminium sample holder with carbon tape and silver paint applied to the area immediately surrounding the sample (to maximise conductivity), and then coated with 5 nm of chromium in a sputter coater (QuorumTechnologies model K575X). Following the coating procedure, samples were introduced into an SEM/Focused Ion Bean (Carl Zeiss – Auriga) with gallium ion bean operated at 30 kV. A region over the cells was milled using 4 nA current. After that, the region exposed by the first milling was polished with 240 pA current and imaged by a backscattering detector with the electron bean operating at 1.5 V. To generate a 3D-surface model, individual high resolution *in situ* cross-section electron micrographs of micropattered cells were stacked using Amira software.

Raman spectroscopy (maps and spectra)

Magnesium fluoride (MgF_2) slides were pre-treated with BD Cell-Tak™ Cell and Tissue Adhesive in a 48-well tissue culture plate (BD Biosciences, 5.2 μL in 300 μL of sodium bicarbonate buffer, pH = 8 for 40 minutes at room temperature). Following two washing steps with ddH_2O, MgF_2 slides were incubated with the cell suspension in PBS for 30 minutes. Slides were then fixed with 4% v/v PFA and washed gently with PBS before analysis. Raman spectral imaging was performed on a confocal Raman microscope (alpha300R+, WITec, Ulm, Germany). A 532 nm laser (Compass Sapphire, Coherent, Gottingen, Germany) was used for excitation. The laser beam was focused through a 63×/1.0 NA water immersion microscope objective lens (W Plan-Apochromat, Zeiss, Oberkochen, Germany). The Raman spectroscopy signals were dispersed by a grating (600 g mm^{-1}) spectrograph (UHTS 300, WITec, Ulm, Germany) and the spectra acquired with a thermoelectrically cooled CCD detector (Newton DU970N-BV-353, Andor, Belfast, UK) with a spectral resolution of 3 cm^{-1}. Raman spectroscopy images ~150 × 150 μm were produced with 400 nm spatial resolution, 1 s integration time and one accumulation per pixel. Spectral collection was centered at 2000 cm^{-1} (0–3000 cm^{-1}). The Control FOUR software (version 4.0, WITec) was used for measurement and Project FOUR Plus (version 4.0, WITec) for spectral data processing.

Clinical plasma sample analysis

Previously collected plasma samples from 22 intensive care unit patients suffering from either from non-infectious (n = 14), infectious SIRS (n = 8) were analysed (Patient characteristics and inclusion/exclusion criteria can be found in the ESI Tables S1 and S2†). All assays were carried out in duplicate (two technical repeats). Blood samples had been collected from an indwelling line into a Heparin Vacutainer tube (5 mL) and stored on ice (maximum 5 minutes) until the first centrifugation step carried out at 2000*g* for 10 minutes.

Plasma biomarker measurement

Procalcitonin (PCT) levels were measured in all samples by enzyme-linked immunoassay (ELISA, Abcam) following the manufacturer's instructions.

Characterization of plasma samples

Plasma samples were pre-processed by centrifugation at 3000*g* for 30 minutes and filtration through a 5 μm filter (Millex Filter Unit, Millipore) in order to remove cell debris. Where indicated, microvesicles were isolated from plasma samples by ultracentrifugation (diluted 1 : 100 in filtered HBSS, 100 000*g* for 1 hour at 4 °C, Beckman Ultracentrifuge). The isolated microvesicles were re-suspended in the same volume of filtered HBSS as the original plasma volume. Plasma samples and samples containing isolated microvesicles were stored at −80 °C, and repeated freeze–thaw cycles were avoided. The plasma protein content of ultracentrifuged samples was below 1% (v/v). Blood count, temperature, heart rate, and C-reactive Protein levels (CRP) were available for all patients included in this study.

Microvesicle characterization – plasma samples

For NTA, plasma samples were analysed directly or following ultracentrifugation using the same camera level (CL 13) for all samples. For flow cytometry, filtered plasma samples were diluted 1 : 10 in triple-filtered phosphate buffered saline (100 nm filter unit, Millipore) and stained following the procedure described above. Double-stained and unstained plasma samples were analysed using the same gating and post-processing (Triton X lysis) procedures as described above for the analysis of *in vitro* samples. Double positive events were counted in the microvesicle gate (events ≤1 μm beads) using counting beads (CountBright, LifeTechnologies).

Microvesicle-based functional activity assays. inflammatory response assay

For the inflammatory response assay, human umbilical vein endothelial cells (HUVEC, Lonza) were seeded in 48-well plates at 25 000 cells per well in endothelial cell growth medium (EGM) supplemented with 10% v/v fetal bovine serum (FBS).

 This journal is © The Royal Society of Chemistry 2015

Open Access Article. Published on 06 July 2015. Downloaded on 7/19/2025 11:24:58 PM.
This article is licensed under a Creative Commons Attribution 3.0 Unported Licence.

For the experiment, FBS-free, phenol red-free endothelial cell basal medium (EBM) was used. Part of the wells were stimulated with 0.1 and 1 μg mL^{-1} LPS (positive controls). Isolated microvesicles were then added to the wells and incubated for 24 hours at 37 °C. LDH release in the supernatants was measured using the Non-Radioactive Cytotoxicity Assay Kit (Promega UK, Southampton , UK). Inflammatory response was quantified using a multiplex cytokine assay kit (4-plex kit, Quansys Biosciences, Logan, UT).

Procoagulant activity assay

The procoagulant activity of microvesicles was measured using a commercially available ZYMUPHEN MP Activity Kit (Aniara, West Chester, OH) and a plasma clotting time assay. For the ZYMUPHEN MP Activity Assay, plasma samples were diluted 1 : 20 and incubated in an AnnexinV coated 96-well plate. Following a washing step, Factor Xa-Va, calcium and prothrombin were added. The phospholipid-induced prothrombin-thrombin activation was measured using a thrombin substrate and absorbance was measured at 405 nm using a plate reader. For the plasma clotting time assay, citrated platelet free plasma from a healthy volunteer was centrifuged at 100 000*g* for 1 hour at 4 °C in order to sediment microvesicles. The microvesicle-free plasma was then added to a 96-well plate (100 μL per well). Five microliter of isolated microvesicles from patient samples were added to each well and incubated for 15 minutes at 37 °C. Following incubation, the citrate plasma was re-calcified by adding 65 μL per well of 50 mM calcium chloride solution and fibrinogen-fibrin polymerization was observed at 405 nm using a plate reader (kinetic measurement, for 100 minutes, 1 measurement per 30 seconds, at 37 °C). Plasma with HBSS was used as negative control, plasma plus amorphous silica nanoparticles (1 mg mL^{-1}) served as positive control.

Bacteria aggregation assay

S. aureus bacteria were stained using a SYTO 9 green fluorescent nucleic acid dye (Invitrogen) following the manufacturer's protocol and diluted to $OD_{600} \sim 1$. For the bacteria aggregation assay, isolated microvesicles were then mixed with the stained bacteria standard in a 10 : 1 volume ratio and incubated at 37 °C for 30 minutes in a glass chamber slide (IBIDI, 8 well chamber slide). Bacteria aggregation was imaged using a confocal microscope (Leica SP5, 20× dry objective). Bacteria aggregates larger than >5 μm were counted using ICY/Image J.

Animal samples

Stored heparinised plasma samples from 12 Wistar rats (Charles River Laboratories Inc.) that underwent CLP (midline laparotomy, 10% ligation of the cecum, single puncture with a 18G needle) and 10 SHAM rats (midline laparotomy, luxation of cecum, incision of ligament, reposition) were obtained from different time points: 0, 24, 48, 72 and 96 hours after surgery. The plasma had been prepared by centrifuging the collected blood at 2500*g*, for 10 minutes at 4 °C, filtration through a 5 μm filter (Millex Filter Unit, Millipore) and samples had been stored at −80 °C. Microvesicle analysis was performed as described above. For flow cytometry, FITC mouse anti-rat CD18 (WT3, IgG1, AbD Serotec) and Alexa-647 anti-rat CD11β (OX-42, IgG2a, κ, BioLegend) were used for double staining at a concentration of 1 μg mL^{-1}.

Microfludic chip

A weir-filter polycarbonate chip with weir-filter slit heights of 5, 10 and 20 μm and pipette adapters were purchased (Microfluidic Chip Shop, Jena, Germany). The samples containing isolated microvesicle were incubated with serum-opsonised *S. aureus* bioparticles for 30 minutes and filtered through the weir-filter chip. The fluorescence intensity (488 nm excitation, 530 nm emission) was measured at the chip inlet and the outlet immediately after, resulting in a total time-to-result (including the microvesicle isolation step) of 1.5 hours.

Statistics

Two groups (control group *versus* sepsis patients or SHAM *versus* CLP) were compared using the Mann-Whitney-U test (two-sided). ROC curves were calculated for the two groups based on the clinical classification. AUC values were extracted and analysed using the ROC tool in MedCalc/Origin. For correlation analyses, Spearman's rho coefficients (pair-wise) were calculated in Origin. *p*-Values <0.05 were considered statistically significant.

Acknowledgements

We thank Ms. Rachael Harrison, Dr Paola Campagnolo, Dr Kieran O'Dea and Prof. Dr Beatrice Beck-Schimmer for helpful discussions. Microscopy was performed in the Facility for Imaging by Light Microscopy (FILM) at Imperial College London. I.K.H. received financial support from the Swiss National Science Foundation (grant number: 145756). S.B. acknowledges a Junior Research Fellowship from Imperial College London. D.O.C received support from the Intensive Care Foundation in the form of a young investigators award. The clinical sample collection was funded by an Intensive Care Foundation Young Investigator Award and the National Institute for Health Research (NIHR) supported it through the Comprehensive Biomedical Research Centre based at Imperial College Healthcare NHS Trust and Imperial College London, and the infrastructure provided by the Critical Care Specialty Group of the Comprehensive Clinical Research Network. Dr Gordon is an NIHR Clinician Scientist Fellowship award holder. M.M.S. thanks EPSRC grant EP/K020641/1.

Notes and references

1 G. S. Martin, D. M. Mannino, S. Eaton and M. Moss, *N. Engl. J. Med.*, 2003, **348**, 1546–1554.
2 J. L. Vincent, in *Sepsis and Non-infectious Systemic Inflammation*, eds. J. M. Cavaillon and C. Adrie, WILEY-VCH Verlag GmbH & Co. KGaA, Weinheim, Germany, 2009.

Open Access Article. Published on 06 July 2015. Downloaded on 7/19/2025 11:24:58 PM.
This article is licensed under a Creative Commons Attribution 3.0 Unported Licence.

3 N. C. Riedemann, R.-F. Guo and P. A. Ward, *J. Clin. Invest.*, 2003, **112**, 460–467.
4 D. C. Angus, W. T. Linde-Zwirble, J. Lidicker, G. Clermont, J. Carcillo and M. R. Pinsky, *Crit. Care Med.*, 2001, **29**, 1303–1310.
5 M. J. Llewelyn, M. Berger, M. Gregory, R. Ramaiah, A. L. Taylor, I. Curdt, F. Lajaunias, R. Graf, S. J. Blincko, S. Drage and J. Cohen, *Crit. Care*, 2013, **17**, R60.
6 R. P. Dellinger, M. M. Levy, J. M. Carlet, J. Bion, M. M. Parker, R. Jaeschke, *et al.*, *Crit. Care Med.*, 2008, **36**, 296–327.
7 I. Jawad, I. Luksic and S. B. Rafnsson, *J. Global Health*, 2012, **2**, 10404.
8 C. Pierrakos and J.-L. Vincent, *Crit. Care*, 2010, **14**, R15.
9 K. L. Becker, R. Snider and E. S. Nylen, *Crit. Care Med.*, 2008, **36**, 941–952.
10 C. Wacker, A. Prkno, F. M. Brunkhorst and P. Schlattmann, *Lancet Infect. Dis.*, 2013, **13**, 426–435.
11 R. Laxminarayan, A. Duse, C. Wattal, A. K. M. Zaidi, H. F. L. Wertheim, N. Sumpradit, *et al.*, *Lancet Infect. Dis.*, 2013, **13**, 1057–1098.
12 M. Baron, C. M. Boulanger, B. Staels and A. Tailleux, *J. Cellular Mol. Med.*, 2012, **16**, 1365–1376.
13 P. S. Prakash, C. C. Caldwell, A. B. Lentsch, T. A. Pritts and B. R. H. Robinson, *J. Trauma Acute Care Surg.*, 2012, **73**, 401–407.
14 V. L. Reid and N. R. Webster, *Br. J. Anaesth.*, 2012, **109**, 503–513.
15 C. I. Timár, A. M. Lorincz, R. Csepanyi-Koemi, A. Valyi-Nagy, G. Nagy, E. I. Buzas, Z. Ivanyi, A. Kittel, D. W. Powell, K. R. McLeish and E. Ligeti, *Blood*, 2013, **121**, 510–518.
16 S. Oehmcke, J. Westman, J. Malmstrom, M. Morgelin, A. I. Olin, B. Kreikemeyer and H. Herwald, *PLoS Pathog.*, 2013, **9**(8), e1003529.
17 C. M. Boulanger and F. Dignat-George, *Arterioscler., Thromb., Vasc. Biol.*, 2011, **31**, 2–3.
18 S. F. Mause and C. Weber, *Circ. Res.*, 2010, **107**, 1047–1057.
19 E. Letsiou, S. Sammani, W. Zhang, T. Zhou, H. Quijada, L. Moreno-Vinasco, S. M. Dudek and J. G. N. Garcia, *Am. J. Respir. Cell Mol. Biol.*, 2015, **52**, 193–204.
20 S. O. Konorov, H. G. Schulze, C. G. Atkins, J. M. Piret, S. A. Aparicio, R. F. B. Turner and M. W. Blades, *Anal. Chem.*, 2011, **83**, 6254–6258.
21 J. M. Robinson, M. L. Karnovsky and M. J. Karnovsky, *J. Cell Biol.*, 1982, **95**, 933–942.
22 K. Doi, A. Leelahavanichkul, P. S. T. Yuen and R. A. Star, *J. Clin. Invest.*, 2009, **119**, 2868–2878.
23 D. Rittirsch, M. S. Huber-Lang, M. A. Flierl and P. A. Ward, *Nat. Protocols*, 2008, **4**, 31–36.
24 C. Timár, Á. Lőrincz and E. Ligeti, *Pfluegers Arch.*, 2013, **465**, 1521–1533.
25 C. A. Arias and B. E. Murray, *N. Engl. J. Med.*, 2009, **360**, 439–443.
26 K. Morris, *Lancet*, 2008, **372**, 1941–1942.
27 I. K. Herrmann, M. Urner, M. Hasler, B. Roth-Z'Graggen, C. Aemisegger, W. Baulig, E. K. Athanassiou, S. Regenass, W. J. Stark and B. Beck-Schimmer, *Nanomedicine*, 2011, **6**(7), 1199–1213.
28 B. György, T. G. Szabó, L. Turiák, M. Wright, P. Herczeg, Z. Lédeczi, A. Kittel, A. Polgár, K. Tóth, B. Dérfalvi, *et al.*, *PLoS One*, 2012, **7**(11), e49726.

This journal is © The Royal Society of Chemistry 2015